



Contents lists available at ScienceDirect

Journal of South American Earth Sciences

journal homepage: www.elsevier.com/locate/jsames

Lu–Hf isotope evidence for the provenance of Permian detritus in accretionary complexes of western Patagonia and the northern Antarctic Peninsula region

C. Mark Fanning^{a,*}, Francisco Hervé^{b,f}, Robert J. Pankhurst^c, Carlos W. Rapela^d, Laura E. Kleiman^e, Greg M. Yaxley^a, Paula Castillo^b

^a Research School of Earth Sciences, The Australian National University, Canberra, Australia

^b Departamento de Geología, Universidad de Chile, Plaza Ercilla 803, Santiago, Chile

^c Visiting Research Associate, British Geological Survey, Keyworth, Nottingham, UK

^d Centro de Investigaciones Geológicas, Calle 1, No. 644, La Plata, Argentina

^e Gerencia de Exploración de Materias Primas, Comisión Nacional de Energía Atómica, Avda. del Libertador 8250, 1419 Buenos Aires, Argentina

^f Escuela de Ciencias de la Tierra, Universidad Andres Bello, Santiago, Chile

ARTICLE INFO

Article history:

Received 13 September 2010

Accepted 12 March 2011

Keywords:

Zircon

Hf isotopes

Permian

Provenance

Patagonia

Antarctic Peninsula

ABSTRACT

Lu–Hf isotope data are presented for dated Permian zircon grains from six samples of the latest Palaeozoic to Jurassic low-grade metasedimentary rocks of western Patagonia and the northern Antarctic Peninsula, as well as from potential source rocks in the North Patagonian Massif. The results for the metasedimentary rocks yield ϵ_{Hf} values mostly between -15 and $+4$ (130 analyses), with a dominant range (more than 85%) of -6 to $+1$, indicating provenance from Permian magmatic rocks that incorporated continental crust with a significant residence time. Other zircon grains record more negative ϵ_{Hf} values indicating derivation from yet more mature crustal sources. Permian subvolcanic granites in the North Patagonian massif appear to be the closest large source area and dated zircon grains from eight samples of these granites yield initial ϵ_{Hf} values of -12 to $+4$ (45 measurements), 84% of which fall between -6 and $+1$, the range shown by the metasediments. However, the North Patagonian massif also contains some more juvenile Permian–Carboniferous components not seen in the metasediments, so that this may not be the primary or unique source. These granites are considered to represent the southernmost extension of the Choiyoi igneous province, which contains abundant Permian rhyolites that crop out on the eastern side of the Andes in central Argentina, for which unpublished Hf isotope data yield a very similar range to that of the metasediments. The widespread nature of the Choiyoi volcanic rocks and the predominance of Permian zircon could make this a more favoured source for the detrital grains.

Hf isotope data reinforce the uniformity of the provenance of the turbidite detrital zircons and confirm the Choiyoi igneous province and the Permian granitic rocks of the North Patagonian Massif as feasible sources. They further confirm the dominantly crustal origin of the Permian magmas. A source region involving mixing of, for example, crustal materials of Panafrican/Brasiliano and Grenvillian ages, together with a minor but significant subduction-related magmatic input, is an isotopically feasible explanation and is broadly consistent with the provenance of pre-Permian crust in this region, but the proportions of such a mixture must have remained relatively constant. This supports the proposal that recently recognised but widespread Permian magmatism in Patagonia represents voluminous crustal melting in response to subducted slab break-off. The results are also consistent with the premise that the Antarctic Peninsula and southern Patagonia were closely located from Permian to Jurassic times, receiving detritus from the same source.

© 2011 Elsevier Ltd. All rights reserved.

1. Introduction

During the late Palaeozoic and/or early Mesozoic turbidites and related sedimentary rocks were notably deposited in accretionary complexes on the present-day Pacific margin of southern Chile (south of 48°S) and a widespread greywacke succession in the

* Corresponding author.

E-mail addresses: mark.fanning@anu.edu.au (C.M. Fanning), fherve@cec.uchile.cl (F. Hervé), rjpankhurst@nigl.nerc.com (R.J. Pankhurst), crapela@cig.museo.unlp.edu.ar (C.W. Rapela), kleiman@cnea.gov.ar (L.E. Kleiman), greg.yaxley@anu.edu.au (G.M. Yaxley), paucasti@ing.uchile.cl (P. Castillo).

Antarctic Peninsula region (Fig. 1b and c). Direct comparison of low-grade metasedimentary rocks of the Duque de York complex (DYC), Trinity Peninsula Group (TPG) and Miers Bluff Formation (MBF) is significant, since in the Gondwana reconstructions of Lawver et al. (1998) and König and Jokat (2006) the Antarctic Peninsula is considered to have been located immediately west of the present-day Patagonian Andes in Triassic to Jurassic times (Fig. 1a). On the basis of these widely cited reconstructions, this relationship would be expected to have applied during deposition of the DYC, TPG and MBF. Hervé et al. (2003, 2005) and Millar et al. (2003) examined the provenance of these turbidites using detrital zircon U–Pb age patterns, which revealed a high proportion of igneous grains of Permian age. On this basis, Hervé et al. (2005) supported the idea of juxtaposition of the Antarctic Peninsula and Patagonian Andes during the time period ~200–145 Ma. Strong petrographic and geochemical similarities between the turbidites of the Trinity Peninsula Group in Antarctica and of the Duque de York complex in western Patagonia, as well as further detrital zircon dating of three additional sandstone samples (Castillo et al., 2009), suggest that these successions derive from a similar source.

Since Permian-age igneous zircons are so predominant in these metasedimentary rocks, there must have been a significant magmatic region exposed and shedding detritus during deposition. Further isotopic characterisation and tracing should allow possible sources to be explored in more detail. With this in mind, we have undertaken Hf isotope analyses on zircon grains whose SHRIMP U–Pb ages were previously determined, both from these metasedimentary rocks

(Hervé et al., 2003; Hervé et al., 2006) and from Permian granitoids of the North Patagonian Massif as a potential source (Pankhurst et al., 2006; see Figs. 1b and 3). Zircons from two samples from the Trinity Peninsula Group of the Antarctic Peninsula have also been analysed for U–Pb SHRIMP age and Hf isotopes for comparison. The Hf isotopic data place constraints on the crustal residence time of the source(s) that yielded the magmas from which these zoned igneous zircons crystallised. They enable us to examine the relative proportions in these magmatic systems of juvenile depleted mantle input and recycled, or longer-lived crustal sources, so that more confident correlations can be proposed for source rocks of appropriate age and isotopic characteristics, with significance for plate tectonic relationships.

2. Analytical methods

Previously dated zircon grains were analysed from three samples from Patagonia (Hervé et al., 2003), one from the Miers Bluff Formation, Livingston Island, South Shetland Islands (Hervé et al., 2006), and two from the Trinity Peninsula Group, Antarctic Peninsula. New SHRIMP U–Pb zircon data for the Trinity Peninsula Group samples, following analytical procedures given in Williams (1998) are presented in Appendix 1. Laser ablation multi-collector inductively-coupled plasma mass-spectrometry (LA-MC-ICMS) Lu–Hf isotopic analyses were carried out at the Research School of Earth Sciences, Australian National University, using a Neptune MC-ICPMS coupled with a HelEx 193 μm ArF Excimer laser ablations

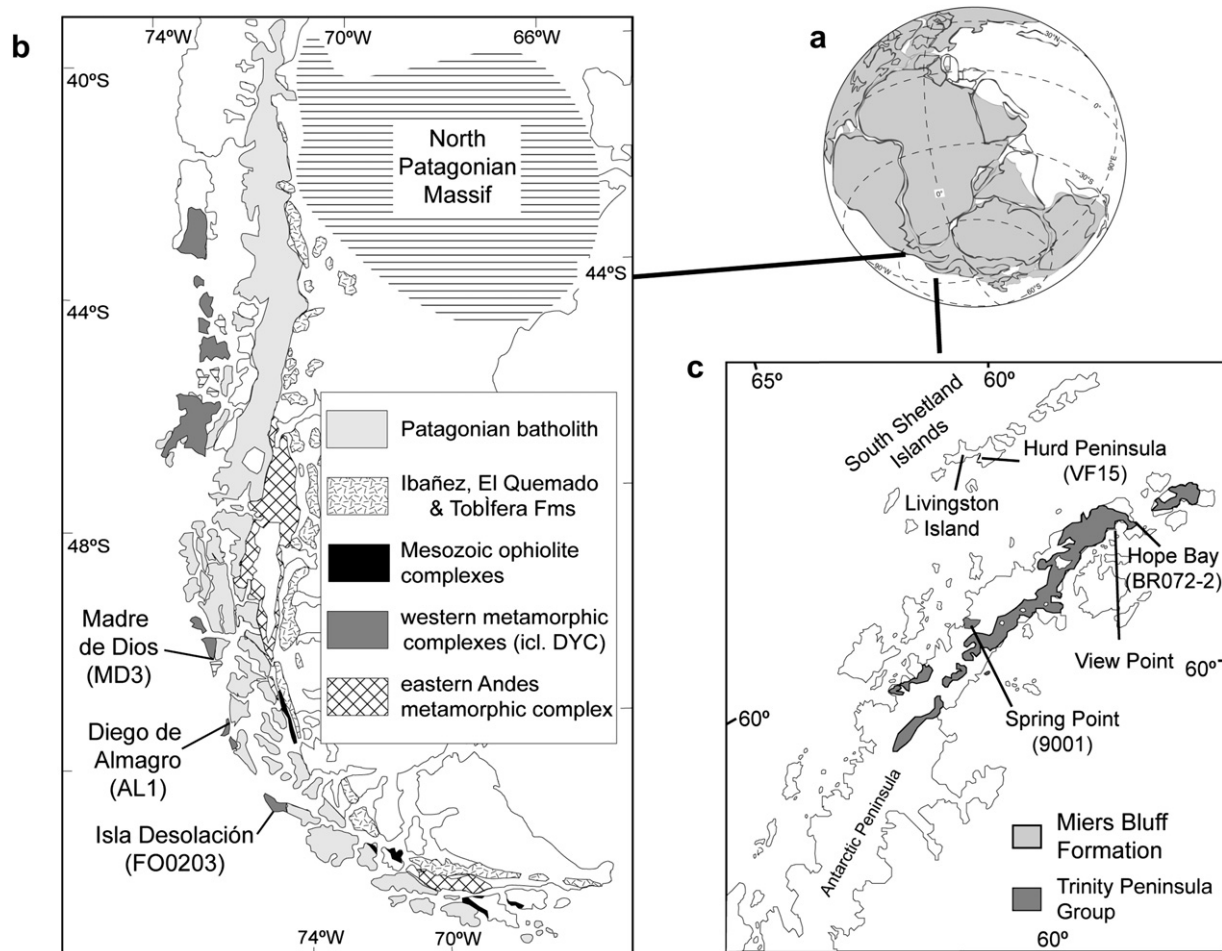
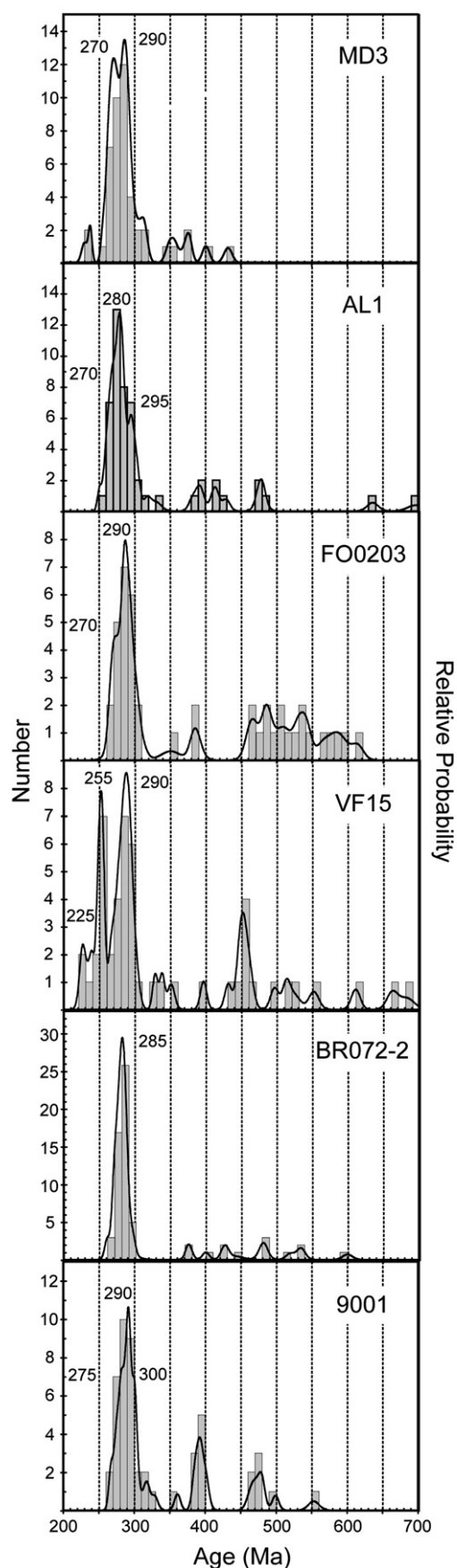


Fig. 1. Location diagram and sketch showing (a) the Gondwana reconstruction of Lawver et al. (1998), (b) localities sampled in western Patagonia and (c) northern Antarctic Peninsula. An enlarged sketch map of the North Patagonian Massif is given in Fig. 3.



system, following procedures described in Munizaga et al. (2008). On the basis of the SHRIMP U–Pb data, Permian-age zircon grains with a simple zoned igneous internal structure were selected. Cathodoluminescence (CL) imaging and transmitted light photomicrographs were used to ensure that analysed domains were of sufficient size to accommodate the ~ 40 to $50 \mu\text{m}$ diameter laser pit, thus ensuring as far as possible that a single-age zircon component was analysed for the Hf isotopic composition. Results are given in Tables 1a, 1b and 2.

3. Samples analysed

3.1. Chilean Patagonia

The Duque de York Metamorphic Complex is a turbiditic succession that is mostly in tectonic juxtaposition with an accreted oceanic island complex of pillow basalt, red and white cherts (Denaro Complex) and Early Permian pelagic fusulinid limestones (Tarlton Limestone) (Forsythe and Mpodzis, 1979). Locally, the Duque de York Metamorphic Complex unconformably overlies the Denaro Complex and Tarlton Limestone (Willner et al., 2009). The youngest U–Pb detrital zircon age of ~ 240 Ma for two grains reported by Hervé et al. (2003) (reproduced in Fig. 2) suggests a Triassic or younger depositional age. However on the basis of further SHRIMP zircon analyses and palynological data, Sepúlveda et al. (2010) suggest an early to middle Permian depositional age. The Duque de York Complex samples analysed here come from the Madre de Dios archipelago (MD3), the Diego de Almagro archipelago (AL1) and Isla Desolación (FO0203) near the western entrance of Magellan Strait (Fig. 1b). The detailed geology and petrography of these samples were reported by Hervé et al. (2003), and Hervé and Fanning (2003). The SHRIMP U–Pb zircon data have been replotted in Fig. 2 to highlight the predominance of detrital zircon ages in the range 270–300 Ma. For sample MD3 the ~ 290 Ma group is slightly more prominent than the ~ 270 Ma group, for sample AL1 ~ 280 Ma is the major age peak with subordinate groups at ~ 295 Ma and ~ 270 Ma. For sample FO0203 ~ 290 Ma is the major age peak with a shoulder at ~ 270 Ma, and it is noteworthy that scattered Palaeozoic grains with ages in the range 450–600 Ma are also present in this sample.

3.2. South Shetland Islands

The Miers Bluff Formation crops out exclusively at Hurd Peninsula on Livingstone Island (Fig. 1c). It is composed of turbiditic sandstone, mudstone, conglomerate and sedimentary breccias. It has been subdivided into the Johnsons Dock and Napier Peak members, which may represent sedimentation in upper and lower mid-fan settings, respectively, prior to pre-late Jurassic polyphase deformation (dominated by open folding) (Smellie et al., 1995). The thickness of the Miers Bluff Formation is believed to be >3000 m (Dalziel, 1969; Arche et al., 1992; Pallás et al., 1992; Smellie et al., 1995), but the base of the formation is unexposed. Petrographic studies (Arche et al., 1992) suggest that the provenance of the turbidites was an active volcanic arc, grading into continental blocks with a source (or sources) on uplifted basement where metamorphic rocks were dominant over plutonic ones. Illite

Fig. 2. Relative probability plot of SHRIMP U–Pb ages for detrital zircons from the analysed samples. Data for MD3 (45 analyses shown from 50 grains analysed in total), AL1 (51 of 56) and FO0203 (43 of 58) have been replotted from Hervé et al. (2003), whereas that for VF15 (50 of 60) is replotted from Hervé et al. (2006). New data presented here for Trinity Peninsula Group samples BR072-2 (64 of 70) and 9001 (49 of 52); see Appendix 1 for data tables.

crystallinity studies indicate very low-grade metamorphism in the anchizone/epizone, predominantly in greenschist facies (Arche et al., 1992; Kelm and Hervé, 1994).

The Miers Bluff Formation was correlated with the Trinity Peninsula Group (Hyden and Tanner, 1981; Aitkenhead, 1975) on the basis of similarities in lithology, and by an assumed relative chronology with respect to other regional geological units. This appeared to be supported by an Early Triassic Rb–Sr isochron age of 243 ± 8 Ma (Willan et al., 1994), but Pimpirev et al. (2002) reported the find of a Tithonian ammonite. Further, Hervé et al. (2006) report the youngest U–Pb detrital zircon age at ~ 225 Ma (Fig. 2; sample VF15) and also note the presence of Jurassic detrital zircons in another sample, consistent with sedimentation into the Late Jurassic.

The SHRIMP U–Pb detrital zircon age data of sample VF15 are replotted for comparison with the other samples discussed in this paper (Fig. 2). Of significance here is the presence of a major age grouping at ~ 290 Ma with another significant group at ~ 255 Ma. Some ~ 450 Ma zircon grains are also present in the detrital age spectrum (Hervé et al., 2006).

3.3. Antarctic Peninsula

Sample 9001 is from a greywacke layer in a turbidite deposit at Spring Point, on the western coast of the Antarctic Peninsula and sample BR072.2 is from a siltstone/mudstone alternation at Scar Hills, Hope Bay (Fig. 1c). Both the sampled rocks are considered to belong to the Trinity Peninsula Group. A Late Palaeozoic depositional age for this group was long assumed but radiometric data are sparse; a Rb–Sr whole-rock errorchron of 281 ± 16 Ma based on suite of samples from Scar Hills that included BR072.2 published by Pankhurst (1983) is considered unreliable, especially since detrital zircons as young as 240 Ma are now shown to be present and fossil evidence suggests that at least part of the Trinity Peninsula Group was deposited during the Triassic (Thomson, 1992). SHRIMP U–Pb data for these samples are given in Appendix 1 and plotted in Fig. 2 for comparison with the other age

spectra. For sample 9001 the dominant age group is at ~ 290 Ma, with a slightly older sub-group at ~ 300 Ma and younger “shoulder” at ~ 275 Ma; BR072.2 shows a single dominant peak at ~ 285 Ma and some minor older provenance. In most respects, but especially in the overwhelming predominance of Permian zircons, these patterns are very comparable to those of the other four samples.

3.4. North Patagonian Massif

U–Pb zircon geochronology of northern Patagonia has been published by Varela et al. (2005) and Pankhurst et al. (2006), showing that the widespread siliceous granitoids that constitute the main outcrops of the Palaeozoic–Mesozoic of the North Patagonian Massif range in age from 294 ± 2 Ma to 257 ± 2 Ma, i.e., throughout the Permian period and extending into the Triassic. Associated volcanic rocks, as well as the composition of the granites, suggests a predominantly subvolcanic environment for emplacement (Llambías and Rapela, 1984), so that this could reasonably be regarded as a subsurface southeasterly extension of the Choiyoi igneous province (e.g., Kay et al., 1989); also termed the Choiyoi rhyolitic province by Kleiman and Japas (2009). Pankhurst et al. (2006) interpret the voluminous and widespread silicic plutonism and volcanism throughout the Permian and into Triassic to be the result of break-off of the subducted plate, with delamination of the lower part of the upper plate, thus allowing access of heat to the overlying Gondwana margin. The zircon samples chosen for this study are from those dated by U–Pb SHRIMP (Pankhurst et al., 2006) that exhibit simple igneous zoning in CL images; samples summarized as below (see Fig 3).

LES-119 is a granodiorite from the Prieto granite, La Esperanza area, in the north of the massif, which has a U–Pb age of 273 ± 2 Ma, an initial ϵ_{Nd} value of -5.0 and an initial $^{87}\text{Sr}/^{86}\text{Sr}$ ratio of 0.7067 .

LES-118 is from the Calvo granite, also in the La Esperanza area, which has a U–Pb age of 250 ± 2 Ma (and could therefore equally

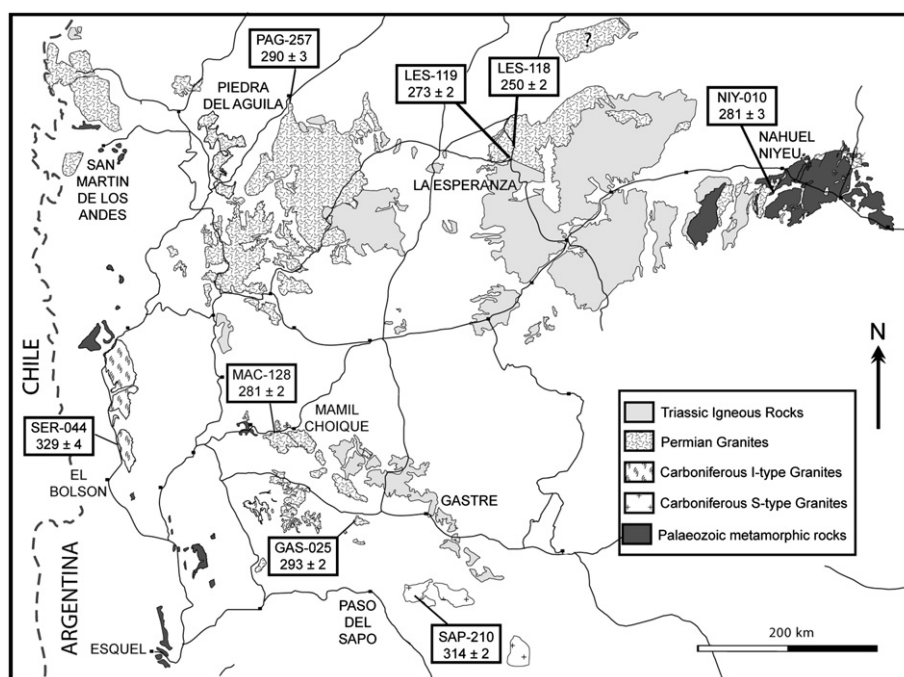


Fig. 3. Sketch map of the North Patagonian Massif modified from Pankhurst et al. (2006) showing the location of the previously U–Pb zircon dated samples used for Hf isotope analyses (note individual sample U–Pb zircon ages given in Ma with 95% confidence limit uncertainties).

Table 1a

Hf isotope data for Permian detrital zircons from Patagonia.

Sample/grain	Age (Ma)	$^{176}\text{Hf}/^{177}\text{Hf}$	± 2 s.e.	$^{176}\text{Lu}/^{177}\text{Hf}$	± 2 s.e.	$\epsilon_{\text{Hf}}(0)$	$\epsilon_{\text{Hf}}(280)$	± 2 s.e.	T_{DM}
MD3: Madre de Dios archipelago, 50°28'S, 75°12.5'W									
1	285	0.282519	0.000021	0.000346	0.000002	-9.40	-3.24	0.74	1420
4	275	0.282495	0.000022	0.001119	0.000039	-10.24	-4.23	0.78	1482
5	264	0.282217	0.000042	0.001199	0.000018	-20.09	-14.10	1.49	2100
6	283	0.282506	0.000039	0.001721	0.000104	-9.87	-3.97	1.37	1466
7	271	0.282518	0.000064	0.001495	0.000061	-9.46	-3.51	2.25	1437
8	274	0.282343	0.000035	0.000402	0.000005	-15.64	-9.50	1.23	1813
9	277	0.282540	0.000023	0.000922	0.000013	-8.68	-2.63	0.80	1381
11	283	0.282518	0.000030	0.000708	0.000029	-9.44	-3.34	1.07	1427
12	270	0.282550	0.000032	0.000763	0.000051	-8.30	-2.22	1.14	1356
14	230	0.282578	0.000027	0.000719	0.000023	-7.33	-1.23	0.96	1294
17	284	0.282584	0.000037	0.000768	0.000030	-7.11	-1.03	1.32	1280
21	265	0.282562	0.000035	0.000472	0.000018	-7.87	-1.74	1.23	1325
22	268	0.282552	0.000034	0.000513	0.000017	-8.23	-2.10	1.20	1348
25	285	0.282506	0.000039	0.000735	0.000019	-9.86	-3.77	1.38	1454
28	265	0.282587	0.000038	0.001233	0.000041	-7.00	-1.00	1.35	1279
29	276	0.282510	0.000024	0.001147	0.000020	-9.71	-3.70	0.84	1449
30	263	0.282524	0.000029	0.000972	0.000022	-9.21	-3.17	1.03	1415
32	289	0.282599	0.000036	0.000565	0.000023	-6.56	-0.44	1.27	1243
34	285	0.282593	0.000034	0.000715	0.000040	-6.79	-0.69	1.19	1259
37	238	0.282525	0.000038	0.000723	0.000060	-9.20	-3.11	1.35	1412
38	263	0.282388	0.000029	0.001068	0.000033	-14.05	-8.02	1.01	1721
39	256	0.282613	0.000037	0.001360	0.000025	-6.07	-0.09	1.32	1221
40	275	0.282487	0.000049	0.000996	0.000072	-10.52	-4.48	1.72	1498
41	269	0.282517	0.000033	0.000641	0.000022	-9.46	-3.36	1.16	1427
44	273	0.282535	0.000035	0.001447	0.000215	-8.85	-2.89	1.25	1398
48	279	0.282543	0.000030	0.000466	0.000012	-8.57	-2.43	1.06	1369
49	279	0.282541	0.000037	0.000810	0.000015	-8.64	-2.57	1.32	1378
AL1: Diego de Almagro archipelago, 51°23.5'S, 75°04.5'W									
1	416	0.282536	0.000026	0.001060	0.000069	-8.82	-2.79	0.94	1391
2	283	0.282585	0.000045	0.000590	0.000027	-7.08	-0.96	1.58	1276
3	636	0.281734	0.000026	0.000625	0.000016	-37.18	-31.09	0.91	3147
5	268	0.282478	0.000028	0.000804	0.000027	-10.85	-4.77	1.01	1517
8	263	0.282469	0.000019	0.000669	0.000035	-11.17	-5.07	0.67	1535
14	296	0.282482	0.000063	0.001028	0.000130	-10.72	-4.69	2.25	1511
15	279	0.282243	0.000046	0.000961	0.000016	-19.17	-13.13	1.62	2039
16	279	0.282613	0.000036	0.000705	0.000027	-6.08	0.02	1.28	1214
17	1249	0.282274	0.000070	0.001337	0.000076	-18.09	-12.11	2.48	1976
18	285	0.282551	0.000023	0.000448	0.000013	-8.27	-2.13	0.81	1350
19	284	0.282552	0.000032	0.000877	0.000042	-8.23	-2.16	1.14	1352
20	284	0.282499	0.000028	0.000343	0.000019	-10.12	-3.96	1.01	1465
21	260	0.282456	0.000072	0.001695	0.000061	-11.63	-5.72	2.55	1576
25	279	0.282524	0.000046	0.001083	0.000028	-9.22	-3.20	1.61	1418
26	263	0.282532	0.000030	0.000456	0.000009	-8.96	-2.82	1.07	1394
29	271	0.282450	0.000037	0.000618	0.000012	-11.84	-5.73	1.32	1577
31	264	0.282516	0.000051	0.001139	0.000025	-9.51	-3.49	1.81	1436
32	274	0.282534	0.000030	0.000755	0.000026	-8.89	-2.80	1.05	1393
36	275	0.282571	0.000032	0.000333	0.000010	-7.58	-1.42	1.13	1305
40	275	0.282456	0.000032	0.000344	0.000011	-11.64	-5.48	1.14	1561
42	252	0.282454	0.000073	0.000430	0.000016	-11.69	-5.54	2.59	1565
43	331	0.282612	0.000063	0.000635	0.000034	-6.12	-0.01	2.22	1216
44	272	0.282454	0.000054	0.001857	0.000100	-11.71	-5.83	1.92	1583
45	298	0.282492	0.000042	0.000860	0.000111	-10.37	-4.30	1.47	1487
46	284	0.282544	0.000056	0.001238	0.000065	-8.53	-2.53	1.98	1376
47	270	0.282568	0.000051	0.000778	0.000033	-7.68	-1.59	1.80	1316
48	285	0.282389	0.000063	0.001986	0.000084	-13.99	-8.13	2.24	1728
49	284	0.282557	0.000060	0.000904	0.000020	-8.07	-2.02	2.12	1343
50	278	0.282493	0.000060	0.001187	0.000060	-10.32	-4.32	2.12	1488
52	273	0.282491	0.000083	0.001208	0.000052	-10.40	-4.40	2.93	1493
53	847	0.282190	0.000043	0.000434	0.000006	-21.04	-14.90	1.51	2150
54	268	0.282578	0.000066	0.000557	0.000050	-7.31	-1.19	2.33	1290
55	282	0.282614	0.000055	0.000686	0.000019	-6.04	0.06	1.96	1212
FO0203: Isla Desolación, 52°56'18.8"S, 74°22'48.8"W									
1	274	0.282546	0.000043	0.000742	0.000013	-8.44	-2.35	1.52	1364
3	271	0.282537	0.000037	0.001073	0.000007	-8.77	-2.75	1.30	1389
23	279	0.282666	0.000032	0.000940	0.000020	-4.21	1.84	1.15	1099
30	282	0.282600	0.000034	0.000862	0.000014	-6.55	-0.49	1.20	1246
32	267	0.282511	0.000034	0.001231	0.000017	-9.71	-3.71	1.22	1450
43	268	0.282572	0.000023	0.000579	0.000010	-7.54	-1.42	0.80	1305
46	276	0.282610	0.000025	0.000544	0.000012	-6.18	-0.05	0.89	1219
50	596	0.282414	0.000025	0.000124	0.000001	-13.11	-6.91	0.89	1651
51	281	0.282573	0.000020	0.000318	0.000005	-7.50	-1.33	0.72	1299
56	279	0.282618	0.000024	0.000440	0.000008	-5.91	0.23	0.87	1201

Table 1b
Hf isotope data for Permian detrital zircons from South Shetland Islands and Antarctic Peninsula.

Sample/grain	Age (Ma)	$^{176}\text{Hf}/^{177}\text{Hf}$	± 2 s.e.	$^{176}\text{Lu}/^{177}\text{Hf}$	± 2 s.e.	$\epsilon_{\text{Hf}}(0)$	$\epsilon_{\text{Hf}}(280)$	± 2 s.e.	T_{DM}
VF15: Miers Bluff, 62°39'44.4"S; 60°23'04.2"W									
4	292	0.282615	0.000063	0.000778	0.000026	-6.02	0.06	2.23	1212
12	271	0.282544	0.000043	0.001023	0.000074	-8.52	-2.48	1.51	1372
15	285	0.282542	0.000040	0.000874	0.000033	-8.59	-2.52	1.43	1375
17	275	0.282646	0.000043	0.000874	0.000015	-4.93	1.13	1.54	1144
19	251	0.282579	0.000048	0.000379	0.000002	-7.28	-1.12	1.70	1286
21	255	0.282330	0.000037	0.001455	0.000092	-16.08	-10.12	1.32	1852
26	282	0.281961	0.000061	0.000671	0.000008	-29.13	-23.04	2.17	2653
27	279	0.282647	0.000052	0.000749	0.000007	-4.90	1.19	1.85	1140
29	266	0.282556	0.000049	0.000642	0.000009	-8.11	-2.00	1.73	1342
31	254	0.282544	0.000047	0.001074	0.000011	-8.53	-2.51	1.68	1374
32	277	0.282561	0.000057	0.000538	0.000021	-7.92	-1.79	2.03	1329
35	251	0.282478	0.000043	0.000621	0.000050	-10.86	-4.76	1.53	1515
44	252	0.282376	0.000045	0.000347	0.000029	-14.46	-8.30	1.59	1738
46	269	0.282370	0.000045	0.001707	0.000040	-14.67	-8.76	1.60	1767
48	256	0.282477	0.000044	0.001435	0.000208	-10.90	-4.94	1.56	1527
50	252	0.282569	0.000034	0.000367	0.000006	-7.64	-1.48	1.19	1309
9001: Spring Point, 64°17'43"S, 61°3'10"W									
1	273	0.282647	0.000042	0.000905	0.000036	-4.87	1.19	1.48	1140
2	289	0.282536	0.000031	0.001298	0.000029	-8.80	-2.81	1.11	1393
9	291	0.282643	0.000018	0.000665	0.000015	-5.03	1.07	0.65	1148
10	290	0.282567	0.000028	0.001071	0.000011	-7.70	-1.67	1.00	1321
14	288	0.282623	0.000027	0.000553	0.000007	-5.73	0.40	0.97	1190
15	293	0.282615	0.000024	0.001637	0.000017	-6.02	-0.09	0.84	1221
18	282	0.282660	0.000036	0.000573	0.000010	-4.43	1.69	1.27	1108
20	285	0.282561	0.000043	0.000922	0.000030	-7.91	-1.85	1.51	1333
23	298	0.282596	0.000020	0.001087	0.000017	-6.70	-0.67	0.70	1258
24	279	0.282684	0.000034	0.000494	0.000015	-3.59	2.55	1.21	1054
25	279	0.282559	0.000034	0.001114	0.000016	-7.99	-1.97	1.21	1340
32	297	0.282575	0.000027	0.001028	0.000064	-7.43	-1.39	0.96	1304
33	281	0.282635	0.000025	0.000787	0.000005	-5.32	0.76	0.90	1167
34	301	0.282533	0.000024	0.000876	0.000021	-8.91	-2.85	0.86	1396
39	284	0.282598	0.000022	0.000477	0.000014	-6.61	-0.47	0.76	1245
40	277	0.282524	0.000028	0.001457	0.000018	-9.22	-3.26	0.98	1421
43	287	0.282673	0.000024	0.000674	0.000014	-3.97	2.13	0.85	1081
44	291	0.282469	0.000036	0.001326	0.000051	-11.18	-5.20	1.27	1543
45	276	0.282513	0.000024	0.000829	0.000015	-9.63	-3.55	0.85	1440
47	265	0.282605	0.000027	0.001843	0.000052	-6.36	-0.48	0.97	1246
BR 072.2: Hope Bay, coastal outcrop, Scar Hills, central Hope Bay									
1	285	0.282533	0.000030	0.000510	0.000013	-8.93	-2.80	1.05	1392
2	284	0.282578	0.000023	0.000436	0.000005	-7.31	-1.16	0.82	1289
6	299	0.282540	0.000021	0.001672	0.000044	-8.68	-2.76	0.74	1390
12	282	0.282549	0.000032	0.001274	0.000037	-8.36	-2.37	1.13	1365
20	287	0.282614	0.000022	0.000699	0.000026	-6.04	0.06	0.79	1212
21	277	0.282611	0.000025	0.000466	0.000002	-6.16	-0.02	0.88	1217
26	287	0.282567	0.000022	0.001566	0.000033	-7.70	-1.77	0.77	1327
28	534	0.282293	0.000024	0.001317	0.000061	-17.40	-11.43	0.86	1934
29	277	0.282592	0.000032	0.000481	0.000020	-6.81	-0.67	1.13	1258
30	288	0.282577	0.000026	0.001124	0.000016	-7.37	-1.35	0.91	1301
33	281	0.282571	0.000022	0.000547	0.000006	-7.57	-1.44	0.78	1307
34	275	0.282459	0.000039	0.001415	0.000108	-11.53	-5.57	1.37	1567
36	292	0.282497	0.000023	0.000551	0.000042	-10.20	-4.07	0.80	1473
37	282	0.282495	0.000047	0.000951	0.000046	-10.25	-4.21	1.66	1481
38	271	0.282543	0.000025	0.001005	0.000019	-8.55	-2.51	0.89	1374
42	280	0.282577	0.000024	0.000626	0.000012	-7.37	-1.26	0.84	1295
44	279	0.282496	0.000029	0.000748	0.000005	-10.22	-4.13	1.02	1476
46	281	0.282555	0.000022	0.000347	0.000006	-8.12	-1.96	0.77	1339
47	289	0.282616	0.000039	0.002375	0.000183	-5.99	-0.21	1.37	1229
48	289	0.282568	0.000021	0.000882	0.000041	-7.67	-1.60	0.75	1317
53	270	0.282562	0.000025	0.000735	0.000010	-7.87	-1.78	0.90	1328
55	279	0.282546	0.000020	0.000736	0.000013	-8.44	-2.35	0.72	1364
61	273	0.282541	0.000019	0.001011	0.000021	-8.61	-2.58	0.68	1378
62	285	0.282591	0.000025	0.001001	0.000032	-6.87	-0.83	0.88	1268

Notes: grains older than Permian are shown in italics; ^{176}Lu decay constant from Söderlund et al. (2004); chondritic values from Bouvier et al. (2008); present-day Depleted Mantle values from Vervoort & Blichert-Toft (1999); bulk earth $^{176}\text{Lu}/^{177}\text{Hf}$ ratio of 0.015 from Goode & Vervoort (2006).

be earliest Triassic) and an initial ϵ_{Nd} value of -7.7 consistent with its S-type chemistry (an apparent initial $^{87}\text{Sr}/^{86}\text{Sr}$ ratio of 0.7036 is considered unreliable due to its high Rb/Sr ratio).

NIY-010 is a granodiorite from south of Nahuel Niyeu in the east of the massif, which has a U–Pb age of 281 ± 3 Ma, an initial ϵ_{Nd} value of -2.1 , and an initial $^{87}\text{Sr}/^{86}\text{Sr}$ ratio of 0.7047.

MAC-128 is a granodiorite from west of Mamil Choique in the west of the massif, which has a U–Pb age of 281 ± 2 Ma, an initial ϵ_{Nd} value of -4.5 , and an initial $^{87}\text{Sr}/^{86}\text{Sr}$ ratio of 0.7068.

GAS-025 is a granodiorite from near Gastre in the southwest of the massif, which has a U–Pb age of 273 ± 2 Ma, an initial ϵ_{Nd} value of -3.6 , and an initial $^{87}\text{Sr}/^{86}\text{Sr}$ ratio of 0.7067.

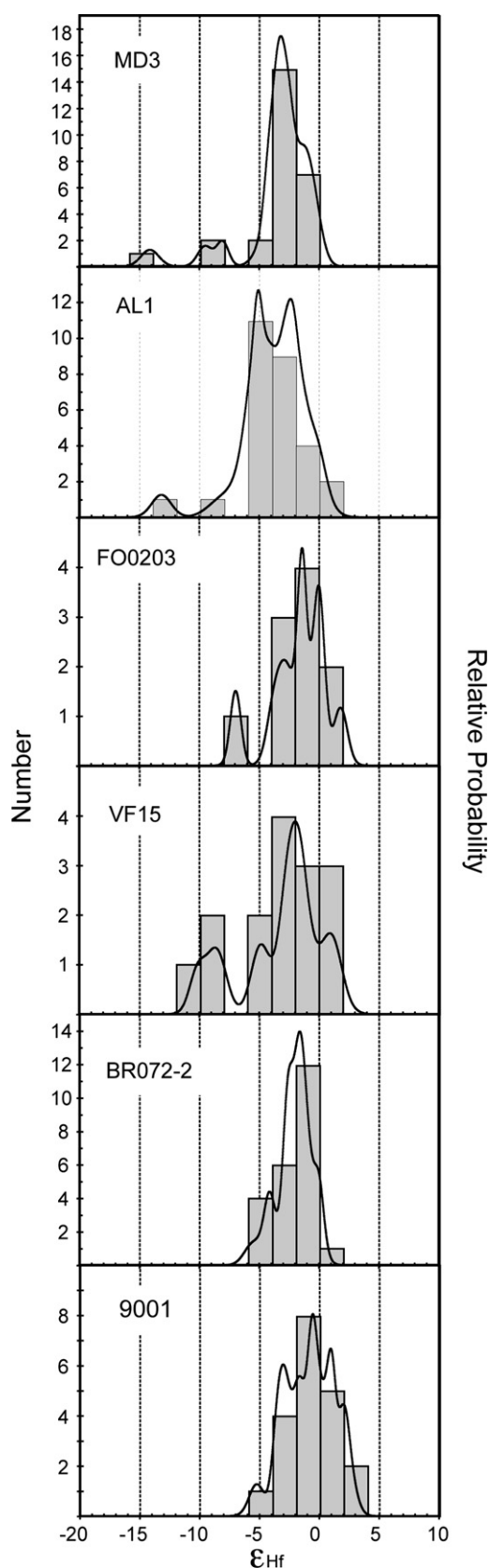


Fig. 4. Histograms and relative probability curves for the initial ϵ_{Hf} values, calculated at 280 Ma, for zoned igneous detrital zircon grains of Permian age in the analysed samples.

PAG-257 is a granite from Piedra del Aguila in the extreme northwest of the massif. It has a U–Pb zircon age of 290 ± 3 Ma, but no Nd or Sr isotope data are available.

In addition, igneous zircon from two Carboniferous samples has also been analysed. Sample SAP-210 is a foliated hornblende granodiorite from east of Paso del Sapo with a U–Pb age of 314 ± 2 Ma, an initial ϵ_{Nd} value of -5.5 , and an initial $^{87}\text{Sr}/^{86}\text{Sr}$ ratio of 0.7076. Sample SER-044 is a foliated granodiorite from Cascada de la Virgen with a U–Pb age of 330 ± 4 Ma, an initial ϵ_{Nd} value of $+1.2$, and an initial $^{87}\text{Sr}/^{86}\text{Sr}$ ratio of 0.7046. It is notable that this latter sample has a significantly higher initial ϵ_{Nd} than all other samples analysed from the North Patagonian Massif – Pankhurst et al. (2006) identified SAP-210 and SER-044 as representative of penecontemporaneous S-type and I-type suites, respectively.

4. Lu–Hf isotopic results

The results of the Lu–Hf isotopic analyses (Tables 1a and 1b) are plotted in Fig. 4 and their main features are described below.

4.1. Chilean Patagonia

Twenty four of the 27 Permian-age zircon grains analysed from sample MD3, have calculated initial ϵ_{Hf} values at 280 Ma between 0 and -4 , with three grains exhibiting more negative values down to -14 (Table 1a, Fig. 4). For sample AL1 from the Diego de Almagro archipelago, 24 of 28 Permian grains analysed have ϵ_{Hf} values between 0 and -6 , another two have barely positive ϵ_{Hf} values (~ 0.05) and a further two grains have values ranging down to -13 . Five older grains with U–Pb ages up to ~ 1245 Ma were also analysed from this sample; they record the presence of significantly more negative initial ϵ_{Hf} values. The sample from Isla Desolación (FO0203) has a grouping of ϵ_{Hf} values between $+2$ and -4 for 8 of the 9 Permian grains analysed. One older Palaeozoic grain was also analysed.

Overall, the Patagonian samples mostly record ϵ_{Hf} values in the range 0 to -5 for Permian zoned igneous zircon (calculated at a common age of 280 Ma) (Fig. 4). At this time the depleted mantle would have had an ϵ_{Hf} of about $+15$. The calculated two-stage depleted mantle model ages for these grains are consistently in the range ~ 1000 to 2000 Ma (Table 1a) indicating a source (or sources) with a significant previous crustal residence time, or a variable mixture of significantly older crust (Proterozoic–Archaean) and more juvenile Palaeozoic material.

4.2. South Shetland Islands and Antarctic Peninsula

The 15 Permian grains analysed from the Miers Bluff Formation on Livingston Island (sample VF15) have ϵ_{Hf} values between $+1.2$ and -10 (Table 1b, Fig. 4). The distribution and range is wider than seen in the Patagonian samples, although 12 of the 15 analyses are in the more restricted range $+1.2$ to -5 , similar to that noted above. Twenty grains have been analysed from the Trinity Peninsula Group sample at Spring Point (9001) and the ϵ_{Hf} values are all in the range $+2.6$ to -5.2 , overlapping with those of sample VF15. The 23 Permian grains analysed from the Hope Bay Trinity Peninsula Group sample BR072–2 are in the range 0 to -5.6 , in complete overlap with the other two samples.

4.3. North Patagonian Massif

Five analysed grains from the granodiorite LES-119 give a tight group of initial ϵ_{Hf} values of -3.7 to -2.8 (Table 2, Fig. 5), whereas the range for six grains from the granite LES-118 is appreciably more negative at -6.4 to -4.0 in accordance with its more negative

initial ϵ_{Nd} . In contrast, NIY-010, shows a wide range initial ϵ_{Hf} from -3.6 to $+3.2$, and is notable as the only Permian sample showing initial ϵ_{Hf} values around zero. The Permian zircons from MAC-128 and PAG-257 have values restricted to the range -4.2 to -2.3 and -5.5 to -2.2 , respectively, concentrated at about -3 . Five analyses from GAS-025 have initial ϵ_{Hf} values of -2.3 to -0.1 . Overall for the 39 Permian zircon grains analysed, 29 of the initial ϵ_{Hf} values (74%) fall between -5 and 0 (Fig. 5), which is the predominant range for the detrital zircons. The Late Carboniferous S-type granite SAP-210 also has slightly negative initial ϵ_{Hf} values of -3.5 to -0.1 , whereas the I-type SER-044 is distinct from all the other samples in having uniformly positive values of $+1.5$ to $+3.6$, indicating a more depleted magma source.

5. Discussion and conclusions

Although Patagonia and the Antarctic Peninsula are today separated by Drake Passage and the Scotia Sea, U–Pb age spectra for detrital zircons in turbiditic sandstones in the Duque de York Complex, the Miers Bluff Formation and the Trinity Peninsula Group suggest a similar source area (Fig. 2). Permian-age detrital zircons predominate in all of the samples analysed and from petrographic and geochemical analyses Faúndez et al. (2002) suggested that the host turbidites were deposited in an active margin tectonic setting, most probably derived from a subduction-related magmatic arc. A prime candidate is the Choiyoi igneous province and this and other possibilities are considered below.

5.1. Spatial distribution of Permian igneous rocks

Within the Choiyoi siliceous large igneous province Kleiman and Japas (2009) describe a thick sequence mainly of rhyolitic ignimbrites well developed on the eastern side of the Andes near San Rafael. Arc-related sequences, syntectonic with transpression of the San Rafael orogeny (Lower Choiyoi of Kleiman and Japas, 2009) were dated at ~ 281 Ma and were followed by intraplate, postorogenic suites of the upper Choiyoi, spanning from ~ 265 Ma to ~ 252 Ma (SHRIMP U–Pb zircon, Rocha-Campos et al., 2006, 2011).

The volcanic rocks of the Choiyoi thin southwards towards northern Patagonia, where the widespread Permian to Triassic granites of the North Patagonian Massif (Varela et al., 2005; Pankhurst et al., 2006) could be regarded as a further, deeper, extension of the Choiyoi magmatic arc, inboard of the deposition of the accretionary wedge turbidites (Fig. 6), and swinging to a SW–WNW trend that, according to Kleiman and Japas (2009), continues to the Sierra de la Ventana, where Permian igneous rocks include the intraplate Lopez Lecube syenite with a SHRIMP U–Pb zircon age 258 ± 2 Ma (Pankhurst et al., 2006).

5.2. Spatial distribution of Permian detrital zircons

Permian (and in a few cases Carboniferous) detrital zircons have been described from other late Palaeozoic metasedimentary rocks in Patagonia (Augustsson et al., 2006; Sepúlveda et al., 2010) and the Antarctic Peninsula (Millar et al., 2003; Barbeau et al., 2010). Augustsson et al. (2006) indicate c. 305 Ma as the timing for the initiation of subduction in southern Patagonia, and report younger Permian detrital zircon peaks for a rock inboard of the South Patagonian Batholith at $50^{\circ}30'$ S. It should be noted that the East Andes Metamorphic Complex does contain Permian-age detrital zircons, but these turbidites have a distinctly different sediment source, derived from older continental crust (Faúndez et al., 2002). Sepúlveda et al. (2010) dated a tuffaceous horizon from the Duque de York Complex at the Madre de Dios archipelago with a marked

peak at ~ 270 Ma, as well as a turbidite with a prominent peak of detrital zircons at ~ 290 Ma. Barbeau et al. (2010) report LA-ICP-MS detrital zircon analyses for 6 samples from the Trinity Peninsula Group, all with prominent Permian-age peaks. They use statistical analysis to qualify as robust the affinities of these rocks with those of western Patagonia.

High proportions of Permian–Carboniferous detrital igneous zircons are also seen in parts of the Beacon Supergroup, Transantarctic Mountains (Elliot and Fanning, 2008). In the latter case, the source of these grains is interpreted as a magmatic arc on the West Antarctic flank of the Permian–Triassic foreland basin, and in this context the occurrence of Permian plutonic igneous rocks in the Kohler Range of eastern Marie Byrd Land was cited by Pankhurst et al. (1998). Fildani et al. (2009) present 205 detrital zircon U–Pb SHRIMP ages from the southwestern Karoo basin in South Africa, which span from 295 Ma to 240 Ma, with maximum peaks at 275 Ma, 272 Ma and 266 Ma, a similar range to the rocks studied here. So far no Hf isotopic data have been reported for the above detrital Permian zircons.

5.3. Hf isotope data

The Permian detrital zircon grains from six samples of the accretionary complex metasediments from 50° S to 60° S analysed in this study yield dominant ϵ_{Hf} values in the range $+2$ to -6 , with Hf model ages mostly in the range 1000–1600 Ma (Tables 1a and 1b). These values indicate that the source of these Permian zircons had a significant crustal residence dating back to at least Grenvillian times and that the zircons are therefore not derived solely from a juvenile magmatic source (at 280 Ma depleted mantle would have had a ϵ_{Hf} value of about $+15$). A few older grains from the same samples record more negative Hf isotope signatures, indicating derivation from even more mature crustal sources, or possibly different mixtures of less and more enriched sources. The relative uniformity in range of initial Hf isotope data reinforces the idea that the detrital zircons of the considered western Patagonian and northern Antarctic Peninsula rocks had a common, uniform source. In the Gondwana reconstruction of Lawver et al. (1998) at about 200 Ma (latest Triassic to early Jurassic), and that of König and Jokat (2006) at 167.2 Ma (Mid Jurassic), all the analysed metasedimentary successions would have been in relatively close proximity soon after the time of their deposition (Fig. 4), and we suggest that this was also the case when they were deposited.

The new zircon Hf isotopic data from igneous provinces of Permian age help in constraining the magmatic sources for the detrital zircons studied in this paper. Zircons from Permian granites from the North Patagonian Massif mostly have initial ϵ_{Hf} values of -6 to $+1$ (Tables 1a and 1b), an identical range to the detrital zircon values found in the accretionary complexes. The Hf T_{DM} model ages of, mostly, 1000–1600 Ma are also similar to the range of Nd T_{DM} model ages for these Permian granites (see Pankhurst et al., 2006, Table 2). A very small number of grains have more negative values, again suggesting the survival of isotopic inheritance from even older source material. However, one of the analysed North Patagonian plutonic rocks (NIY-010) contains some zircons with more positive initial ϵ_{Hf} values, up to $+3.2$, that are not seen in the detrital zircon grains, nor are Carboniferous zircons generally common among the metasedimentary rocks. Thus the North Patagonian massif may not be a unique sediment source for the accretionary complexes and the more distant Choiyoi volcanic province may be considered more likely.

Few published Hf data exist so far for the main outcrops of the Choiyoi group. Lu–Hf data for 53 Permian zircon grains from Choiyoi volcanic rocks near San Rafael (Kleiman & Fanning, unpublished) yield initial ϵ_{Hf} values at 280 Ma ranging from $+1.3$

Table 2

Hf isotope data for zircons analysed from North Patagonian Massif granites.

Sample/grain	Age (Ma)	$^{176}\text{Hf}/^{177}\text{Hf}$	± 2 s.e.	$^{176}\text{Lu}/^{177}\text{Hf}$	± 2 s.e.	$\epsilon_{\text{Hf}}(0)$	$\epsilon_{\text{Hf}}(280)$	± 2 s.e.	T_{DM}
LES-118: ~6 km N of La Esperanza, Calvo Granite, 40°19'46"S, 68°26'24"W									
3.2	290	0.282503	0.000031	0.001523	0.000079	-9.96	-4.01	1.09	1469
4.2	249	0.282452	0.000024	0.001222	0.000032	-11.77	-5.77	0.86	1579
5.2	247	0.282451	0.000025	0.001180	0.000022	-11.81	-5.81	0.88	1582
6.2	247	0.282446	0.000028	0.001558	0.000078	-12.00	-6.06	1.00	1598
11.2	302	0.282493	0.000019	0.000691	0.000027	-10.33	-4.24	0.67	1483
14.1	250	0.282434	0.000029	0.000871	0.000028	-12.42	-6.35	1.02	1616
LES-119: ~3 km N of La Esperanza, Prieto Granodiorite, 40°22'50"S, 68°27'29"W									
2.1	267	0.282523	0.000022	0.000557	0.000014	-9.25	-3.13	0.77	1413
3.1	274	0.282534	0.000026	0.000881	0.000044	-8.88	-2.81	0.91	1393
7.1	272	0.282507	0.000022	0.000736	0.000026	-9.81	-3.73	0.79	1451
10.1	267	0.282534	0.000023	0.000698	0.000027	-8.87	-2.77	0.82	1391
18.1	272	0.282522	0.000025	0.000522	0.000012	-9.29	-3.16	0.87	1415
MAC-128: 500 m N of Puesto Quintuleu, foliated granodiorite (Mamil Choique), 41°46'33"S, 70°17'56"W									
1.1	285	0.282520	0.000038	0.000452	0.000013	-9.36	-3.22	1.33	1419
3.1	277	0.282508	0.000025	0.000625	0.000020	-9.81	-3.70	0.90	1449
4.1	286	0.282493	0.000026	0.000372	0.000016	-10.32	-4.16	0.92	1478
5.1	285	0.282530	0.000024	0.000280	0.000003	-9.01	-2.84	0.86	1395
6.1	282	0.282540	0.000022	0.000552	0.000011	-8.66	-2.54	0.77	1376
13.1	1031	0.282272	0.000027	0.000588	0.000012	-18.13	-12.02	0.96	1971
11.1	284	0.282525	0.000031	0.000593	0.000035	-9.20	-3.09	1.09	1410
14.1	290	0.282494	0.000027	0.000542	0.000020	-10.31	-4.18	0.96	1479
15.1	280	0.282544	0.000022	0.000256	0.000012	-8.52	-2.34	0.79	1363
NIY-010: Puesto Navarette, granodiorite, 40°35'33"S, 66°33'54"W									
3.1	268	0.282695	0.000021	0.001113	0.000016	-3.17	2.85	0.75	1035
4.1	280	0.282686	0.000021	0.001035	0.000012	-3.48	2.55	0.74	1054
5.1	462	0.282399	0.000060	0.002923	0.000181	-13.64	-7.96	2.11	1717
11.1	277	0.282604	0.000023	0.001288	0.000010	-6.39	-0.40	0.83	1241
12.1	279	0.282650	0.000022	0.001045	0.000023	-4.78	1.25	0.76	1136
13.1	278	0.282675	0.000019	0.000973	0.000017	-3.88	2.17	0.68	1078
16.1	279	0.282695	0.000019	0.000889	0.000033	-3.19	2.87	0.69	1034
17.1	265	0.282705	0.000022	0.001130	0.000012	-2.84	3.18	0.76	1014
18.1	285	0.282514	0.000023	0.001413	0.000034	-9.58	-3.62	0.80	1444
23.1	1048	0.282500	0.000020	0.001019	0.000050	-10.09	-4.05	0.69	1471
PAG-257: Piedra del Aguila, rotten Bio-Musc granite (Mamil Choique), 40°5'14"S, 70°5'7"W									
2.1	308	0.282536	0.000029	0.000740	0.000003	-8.80	-2.71	1.01	1387
3.1	286	0.282515	0.000031	0.000703	0.000043	-9.55	-3.46	1.10	1434
5.1	287	0.282538	0.000034	0.000373	0.000005	-8.73	-2.57	1.20	1378
8.1	295	0.282531	0.000023	0.000474	0.000006	-8.99	-2.85	0.82	1396
11.1	882	0.282311	0.000031	0.000684	0.000024	-16.76	-10.67	1.10	1886
13.1	293	0.282549	0.000024	0.000460	0.000007	-8.33	-2.19	0.84	1354
14.1	286	0.282513	0.000020	0.000377	0.000005	-9.62	-3.47	0.72	1434
17.1	1812	0.281486	0.000025	0.000945	0.000050	-45.92	-39.89	0.88	3682
21.1	297	0.282458	0.000022	0.000615	0.000005	-11.56	-5.45	0.79	1559
GAS-025: Laguna del Toro, Bio granodiorite, 42°21'22"S, 69°51'47"W									
5.1	300	0.282547	0.000026	0.000784	0.000056	-8.40	-2.32	0.91	1362
11.1	296	0.282558	0.000031	0.000911	0.000009	-8.03	-1.97	1.09	1340
12.1	293	0.282610	0.000027	0.000726	0.000020	-6.18	-0.09	0.94	1221
14.1	293	0.282588	0.000032	0.000584	0.000019	-6.97	-0.85	1.12	1269
18.1	285	0.282547	0.000026	0.000784	0.000056	-8.40	-2.32	0.91	1362
SAP-210: east of Paso del Sapo, foliated Bio-Hnb granodiorite, 42°42'27"S, 69°35'53"W									
1.1	305	0.282512	0.000022	0.000642	0.000013	-9.65	-3.54	0.78	1439
5.1	313	0.282538	0.000034	0.000373	0.000005	-8.73	-2.57	1.20	1378
6.1	316	0.282521	0.000026	0.001057	0.000011	-9.32	-3.29	0.93	1423
7.1	319	0.282553	0.000022	0.000514	0.000010	-8.22	-2.08	0.76	1347
12.1	316	0.282610	0.000027	0.000726	0.000020	-6.18	-0.09	0.94	1221
14.1	317	0.282588	0.000032	0.000584	0.000019	-6.97	-0.85	1.12	1269
SER-044: Cascada de la Virgen, foliated granodiorite, 41°49'43"S, 71°25'7"W									
1.1	331	0.282661	0.000039	0.001963	0.000137	-4.38	1.48	1.36	1122
4.1	334	0.282718	0.000040	0.001624	0.000051	-2.36	3.57	1.41	989
5.1	334	0.282717	0.000038	0.002161	0.000055	-2.41	3.42	1.35	999
7.1	324	0.282689	0.000028	0.002187	0.000027	-3.39	2.44	1.00	1061
10.1	318	0.282704	0.000042	0.001211	0.000019	-2.85	3.16	1.50	1015
14.1	328	0.282714	0.000038	0.001401	0.000077	-2.52	3.45	1.34	997
16.1	326	0.282678	0.000041	0.001240	0.000152	-3.77	2.23	1.44	1074

Notes: as per Table 1b.

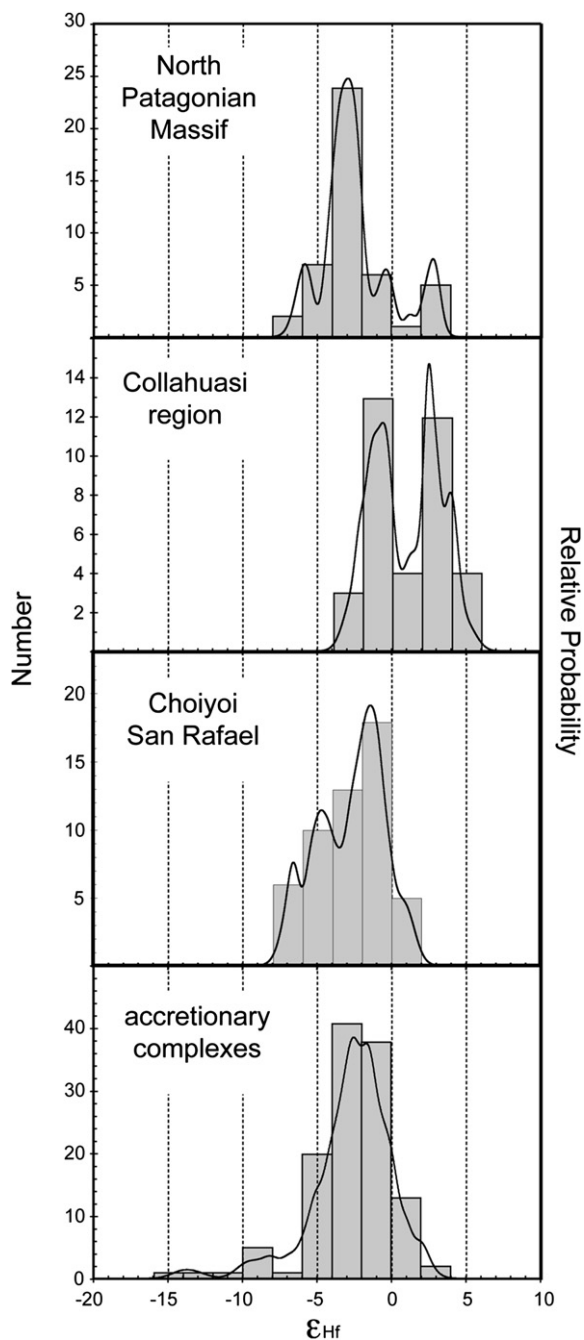


Fig. 5. Composite histograms and relative probability curves for the initial ϵ_{Hf} values, calculated at 280 Ma, for the zoned igneous detrital zircon grains of Permian age in the North Patagonian Massif granite samples and all the accretionary complex sedimentary samples. Comparative curves and histograms are shown for the Choiyoi (Kleiman and Fanning, in preparation) and the Collahuasi (recalculated from Munizaga et al., 2008).

to -7.0 though the majority are between $+1.3$ and -5.5 (47 analyses or 85% of the total). As shown in Fig. 5, this range completely overlaps the values reported here for the accretionary complex detrital zircons. Volcanic rocks from the Collahuasi Formation in northern Chile (23 S. Lat.) (Munizaga et al., 2008), which may be considered a northerly equivalent of the Choiyoi volcanic rocks (Fig. 5), have ϵ_{Hf} values between -2 and $+6$. There is some overlap with the detrital zircon values reported here, but the Collahuasi Permian zircons extend to ϵ_{Hf} values that are even more positive than those from the Permian granites of the North Patagonian



Fig. 6. Reconstruction modified from Lawver et al. (1998), showing the position of the Antarctic Peninsula during the early Jurassic (200 Ma), with indication of the possible source areas for the detrital Permian zircons in Trinity Peninsula Group, Miers Bluff Formation and Duque de York complex, as discussed in this paper. The location of potential sources such as the North Patagonian Massif (NPM) and the Choiyoi Group are shown.

massif and so are not considered as the source for the majority of the detrital Permian zircon grains.

5.4. Nature of the magmatic sources of the Permian precursors of the detrital zircons

The Hf isotope data indicate that neither mantle nor juvenile crust were the main source of the magmatic rocks that contributed Permian zircon to the metasedimentary rocks of western Patagonia and the Antarctic Peninsula. This accords with the isotopic and geochemical evidence for the crustal origin of the Permian igneous rocks of the North Patagonian massif and the Choiyoi province. No such unique source has yet been identified, but rather than a single uniform source there could have been mixing between minor subduction-related components and older continental crust, for example of Panafrican/Brasiliano and Grenvillian age, both of which may be observed as significant in the provenance of pre-Permian metasedimentary rocks in northern Patagonia (Pankhurst et al., 2003). Bahlburg et al. (2009) suggested that the igneous activity in the Central Andean segment of the Terra Australis orogen during the Palaeozoic represents mainly the recycling of Mesoproterozoic continental crust. Other potential crustal sources would include Early Palaeozoic igneous rocks exposed in Patagonia (Pankhurst et al., 2006) or recovered from boreholes in Tierra del Fuego (Söllner et al., 2000; Hervé et al., 2010); the last authors describe a Permian high T /low P high grade metamorphic event which developed migmatitic gneisses in the present basement of the late Mesozoic–Cenozoic Magallanes basin, which implies the formation of Permian silicic melts. However, the corresponding igneous bodies, if they exist, have not yet been detected in this area where removal of several km of rock occurred between the Permian and the Middle Jurassic eruption of the Tobífera silicic volcanic rocks over the gneisses.

Nevertheless, the relative uniformity of the Hf isotope compositions in the Permian magmatic zircons, together with the relative

paucity of older inheritance provenance, requires effective removal of such older zircons and isotopic homogenisation during Permian magma genesis. This is consistent with the proposal that the widespread Permian magmatism in the North Patagonian Massif (NPM) represents large-scale crustal melting in response to post-collisional subducted slab break-off (Pankhurst et al., 2006) and with the Kleiman and Japas (2009) model of slab break-off related to progressive shallowing of the subducting plate towards the Late Permian in the San Rafael region.

5.5. Source areas for detrital zircons

The provenance of the Permian detrital zircons found in the metasedimentary complexes of western Patagonia and the Antarctic Peninsula region from the Permian igneous province of the Central Andes and Patagonia, which includes huge volumes of silicic volcanic rocks and smaller but significant volumes of granitic rocks, seems well established, based on the similarity in age and in Hf isotope composition. At present we cannot discriminate on the basis of U–Pb age and Hf isotopic composition between the zircons of the Permian granites of the North Patagonian Massif and the Choiyoi rovince rhyolites, so that the exact location of the source area of the Permian detrital zircons cannot be precisely pinpointed. If Permian granites were the main zircon source for the accretionary complexes they would have had to be uplifted and eroded rapidly, but this is quite feasible for the high level intrusions of the North Patagonian Massif, which may also have had a volcanic expression. The occurrence of some Early Palaeozoic and older zircons in the detrital patterns of some samples (Fig. 2) is also consistent with this as a possible origin.

Sparse occurrences of Permian granites are also known from the southern parts of the Antarctic Peninsula (Millar et al., 2002), from Marie Byrd Land (Pankhurst et al., 2003) and from the Transantarctic Mountains (Elliot and Fanning, 2008) and could be important as source rocks in those localities. As pointed out by Barbeau et al. (2010), the detrital zircon data reflect a deposition in a terrane parautochthonous to Gondwana, mainly fed in detritus from an active magmatic province, which hindered voluminous sedimentary contributions from the interior of the continent and from the basement of the magmatic deposits.

The similarity in Hf isotope signatures, together with the U–Pb age spectra in the detrital zircons is consistent with the premise that the Antarctic Peninsula was side by side with Patagonia during the Jurassic, receiving detritus from the same source (Fig. 6; Hervé et al., 2006).

The presence of abundant Permian igneous detrital zircons in such different locations as South America (Patagonia, Paraná basin), South Africa (Karoo basin), Antarctica (Antarctic Peninsula and Transantarctic Mountains), only to mention those referred to in this paper, indicates the regional importance in southwestern Gondwana of this magmatic event. Combined detrital zircon and Hf isotopes may help to demonstrate whether the Choiyoi igneous province can be a main source for these deposits.

Acknowledgements

Fondecyt Projects 1050431 and 1095099 and Anillo de Investigación Antártico ARTG-04 from PBCT (CONICYT). Instituto Antártico Chileno (INACH) supported Diego Morata and Elisa Ramírez who collected the sample from Punta Spring during the Chilean Antarctic Scientific Expedition (ECA) in 1999. Captains Conrado Alvarez Jr. and Sr. took us safely to remote areas in the Patagonian archipelago in the yachts *Foam* and *Penguin*, the latter sunk in 2009. We acknowledge the detailed reviews by three anonymous referees that helped to improve the original text.

Appendix A. Supplementary data

Supplementary data associated with this article can be found in the online version at doi:10.1016/j.jsames.2011.03.007.

References

- Aitkenhead, N., 1975. The geology of Duse Bay-Larsen Inlet area, North-East Graham Land (with particular reference to the Trinity Peninsula Series). British Antarctic Survey Scientific Reports 51, 62.
- Arche, A., López-Martínez, J., Marfil, R., 1992. Petrofacies and provenance of the oldest rocks in Livingston Island, South Shetland Islands. In: López-Martínez, J. (Ed.), III Congreso Geológico de España y VIII Congreso Latinoamericano de Geología, Salamanca, España. Geología de la Antártida Occidental, Simposios, T3, pp. 93–104.
- Augustsson, C., Münker, C., Bahlburg, H., Fanning, C.M., 2006. Provenance of late Palaeozoic metasediments of the SW South American Gondwana margin: a combined U–Pb and Hf-isotope study of single detrital zircons. *Journal of the Geological Society, London* 163, 983–995.
- Bahlburg, H., Vervoort, J.D., Du Frane, S.A., Bock, B., Augustsson, C., Reimann, C., 2009. Timing of crust formation and recycling in accretionary orogens: insights learned from the western margin of South America. *Earth-Science Reviews* 97, 227–253.
- Barbeau, D.L., Davis, J.T., Murray, K.E., Valencia, V., Gehrels, G.E., Zahid, K.M., Gombosi, D.J., 2010. Detrital zircon geochronology of the metasedimentary rocks of north-western Graham Land. *Antarctic Science* 22, 65–78.
- Bouvier, A., Vervoort, J.D., Patchett, P.J., 2008. The Lu–Hf and Sm–Nd isotopic composition of CHUR: constraints from unequilibrated chondrites and implications for the bulk composition of terrestrial planets. *Earth and Planetary Science Letters* 273, 48–57.
- Castillo, P., Lacassie, J.P., Hervé, F., Fanning, C.M., 2009. Sedimentary provenance of Trinity Peninsula Group, Antarctic Peninsula: petrography, geochemistry and SHRIMP U–Pb zircon age constraints. *Geophysical Research Abstracts* 11, 3084.
- Dalziel, I.W.D., 1969. Structural studies in the Scotia Arc: Livingston Island. *Antarctic Journal of United States* 4 (194), 137.
- Elliot, D.H., Fanning, C.M., 2008. Detrital zircons from upper Permian and lower Triassic Victoria Group sandstones, Shackleton Glacier region, Antarctica: evidence for multiple sources along the Gondwana plate margin. *Gondwana Research* 13, 259–274.
- Faúndez, V., Hervé, F., Lacassie, J.P., 2002. Provenance studies of pre-late Jurassic metaturbidite successions of the Patagonian Andes, southern Chile. *New Zealand Journal of Geology and Geophysics* 45, 411–425.
- Fildani, A., Weislogel, A., Drinkwater, N.J., McHargue, T., Tankard, A., Wooden, J., Hodgson, D., Flint, S., 2009. U–Pb zircon ages from the southwestern Karoo Basin, South Africa – implications for the Permian Triassic boundary. *Geology* 37 (8), 719–722.
- Forsythe, R.D., Mpodozis, C., 1979. El Archipiélago Madre de Dios, Patagonia Occidental, Magallanes: rasgos generales de la estratigrafía y estructura del basamento pre Jurásico Superior. *Revista Geológica de Chile* 7, 13–29.
- Goode, J.W., Vervoort, J.D., 2006. Origin of mesoproterozoic A-type granites in Laurentia: Hf isotope evidence. *Earth and Planetary Science Letters* 243, 711–731.
- Hervé, F., Fanning, C.M., 2003. Early Cretaceous subduction of continental crust at the Diego de Almagro archipelago, southern Chile. *Episodes* 26, 285–289.
- Hervé, F., Fanning, C.M., Pankhurst, R.J., 2003. Detrital zircon age patterns and provenance in the metamorphic complexes of Southern Chile. *Journal of South American Earth Sciences* 16, 107–123.
- Hervé, F., Miller, H., Pimpirev, C., 2005. Patagonia–Antarctica Connections before Gondwana break-up. In: Fütterer, D.K., Damaske, D., Kleinschmidt, G., Miller, H., Tessensohn, F. (Eds.), *Antarctica: Contributions to Global Earth Sciences*. Springer-Verlag, Berlin Heidelberg New York, pp. 215–226.
- Hervé, F., Faúndez, V., Brix, M., Fanning, M., 2006. Jurassic sedimentation of the Miers Bluff formation, Livingston Island, Antarctica: evidence from SHRIMP U–Pb ages of detrital and plutonic zircons. *Antarctic Science* 18, 229–238.
- Hervé, F., Calderón, M., Fanning, C.M., Kraus, S., Pankhurst, R.J., 2010. The age, nature and significance of the basement rocks of the Magallanes basin in Tierra del Fuego. *Andean Geology* 37, 253–275.
- Hyden, G., Tanner, P.W.G., 1981. Late Palaeozoic–Early Mesozoic fore-arc basin sedimentary rocks at the Pacific margin in western Antarctica. *Geologische Rundschau* 70, 529–541.
- Kay, S.M., Ramos, V.A., Mpodozis, C., Sruoga, P., 1989. Late Paleozoic to Jurassic silicic magmatism at the Gondwana margin: analogy to the Middle Proterozoic in North America? *Geology* 17, 324–328.
- Kelm, U., Hervé, F., 1994. Cristalinidad de la illita en metapelitas del Grupo Península Trinidad, Península Antártica e Isla Livingston: algunas implicancias acerca de su fuente de origen y metamorfismo. *Serie Científica Inach* 44, 9–16.
- Kleiman, L.E., Japas, M.S., 2009. The Choiyoi volcanic province at 34–36S (San Rafael, Mendoza, Argentina): implications for the Late Paleozoic evolution of the southwestern margin of Gondwana. *Tectonophysics* 473, 283–299.

- König, M., Jokat, W., 2006. The Mesozoic breakup of the Weddell Sea. *Journal of Geophysical Research* 111 (B12102), 1–28. doi:10.1029/2005JB004035.
- Lawver, L.A., Gahagan, L.M., Dalziel, I.W.D., 1998. A tight fit Early Mesozoic Gondwana, a plate reconstruction perspective. *Memoirs of the National Institute for Polar Research* 53, 214–229 (special issue) Tokyo.
- Llambías, E.J., Rapela, C.W., 1984. Geología de los complejos eruptivos del Paleozoico superior de La Esperanza, provincia de Río Negro. *Revista de la Asociación Geológica Argentina* 40, 4–25.
- Millar, I.L., Pankhurst, R.J., Fanning, C.M., 2002. Basement chronology of the Antarctic Peninsula: recurrent magmatism and anatexis in the Palaeozoic Gondwana Margin. *Journal of the Geological Society, London* 159, 145–157.
- Millar, I.L., Vaughan, A.P.M., Flowerdew, M.J., Fanning, C.M., Trouw, R.A.J., Bradshaw, J.D., 2003. Provenance of the Trinity Peninsula Group, northern Antarctic Peninsula. In: Fütterer, D.K. (Ed.), *Antarctic Contributions to Global Earth Sciences, Programme and Abstracts. Terra Nostra* 4, 232. Heft.
- Munizaga, F., Maksae, V., Fanning, C.M., Giglio, S., Yaxley, G., Tassinari, C.C.G., 2008. Late Paleozoic–Early Triassic magmatism on the western margin of Gondwana: Collahuasi area, Northern Chile. *Gondwana Research* 13, 407–427.
- Pallás, R., Muñoz, J.A., Sàbat, F., 1992. Estratigrafía de la Formación Miers Bluff, Isla Livingston, Islas Shetland del Sur. In: López-Martínez, J. (Ed.), *III Congreso Geológico de España y VIII Congreso Latinoamericano de Geología, Salamanca, España. Geología de la Antártida Occidental. Simposios, T3*, pp. 105–115.
- Pankhurst, R.J., 1983. Rb–Sr constraints on the ages of basement rocks of the Antarctic Peninsula. In: Oliver, R.L., James, P.R., Jago, J.B. (Eds.), *Antarctic Earth Science. Australian Academy of Science, Canberra*, pp. 367–371.
- Pankhurst, R.J., Weaver, S.D., Bradshaw, J.D., Storey, B.C., Ireland, T.R., 1998. Geochronology and geochemistry of pre-Jurassic superterranes in Marie Byrd Land, Antarctica. *Journal of Geophysical Research* 103B, 2529–2547.
- Pankhurst, R.J., Rapela, C.W., Loske, W.P., Fanning, C.M., Márquez, M., 2003. Chronological study of the pre-Permian basement rocks of southern Patagonia. *Journal of South American Earth Sciences* 16, 27–44.
- Pankhurst, R.J., Rapela, C.W., Fanning, C.M., Márquez, M., 2006. Gondwanide continental collision and the origin of Patagonia. *Earth Science Reviews* 76, 235–257.
- Pimpirev, C., Ivanov, M., Dimov, D., Nikolov, T., 2002. First find of the Upper Tithonian ammonite genus *Blandfordiceras* from the Miers Bluff Formation, Livingston Island, South Shetland Islands. *Neues Jahrbuch für Geologie und Paläontologie* 6, 377–384.
- Rocha-Campos, A.C., Basei, M.A., Nutman, A.P., Kleiman, Laura E., Varela, R., Llambías, E., Canile, F.M., da Rosa, O.C.R., 2011. 30 million years of Permian volcanism recorded in the Choiyoi igneous province (W Argentina) and their source for younger ash fall deposits in the Paraná Basin: SHRIMP U–Pb zircon geochronology evidence. *Gondwana Research* 19, 509–523.
- Rocha-Campos, A.C., Basei, M.A.S., Nutman, A.P., Santos, P.R., 2006. Shrimp U–Pb zircon geochronological calibration of the Late Paleozoic supersequence, Paraná Basin, Brazil. In: *V South American Symposium on Isotope Geology*, pp. 298–301.
- Sepúlveda, F.A., Palma-Heldt, S., Hervé, F., Fanning, C.M., 2010. Constraints for the depositional age of the Duque de York Complex in the allochthonous Madre de Dios Terrane, southern Chile: first palynological record and palaeoclimatic implications. *Andean Geology* 37, 375–397.
- Smellie, J.L., Liesa, M., Muñoz, J.A., Sàbat, F., Pallás, R., Willan, R.C.R., 1995. Lithostratigraphy of volcanic and sedimentary sequences in central Livingston Island, South Shetland Islands. *Antarctic Science* 7, 99–113.
- Söderlund, U., Patchett, J.P., Vervoort, J.D., Isachsen, C.E., 2004. The ^{176}Lu decay constant determined by Lu–Hf and U–Pb isotope systematics of Precambrian mafic intrusions. *Earth and Planetary Sciences Letters* 219, 311–324.
- Söllner, F., Miller, H., Hervé, M., 2000. An Early Cambrian granodiorite age from the pre-Andean basement of Tierra del Fuego (Chile): the missing link between South America and Antarctica? *Journal of South American Earth Sciences* 13, 163–177.
- Thomson, M.R.A., 1992. Stratigraphy and age of the pre-Cenozoic stratified rocks of the South Shetland Islands: a review. In: López-Martínez, J. (Ed.), *III Congreso Geológico de España y VIII Congreso Latinoamericano de Geología, Salamanca, España. Geología de la Antártida Occidental. Simposios, T3*, pp. 75–92.
- Varela, R., Basei, M.A.S., Cingolani, C.A., Siga Jr., O., Passarelli, C.R., 2005. El Basamento Cristalino de los Andes norpatagónicos en Argentina: geocronología e interpretación tectónica. *Revista Geológica de Chile* 32, 167–182.
- Vervoort, J.D., Blichert-Toft, J., 1999. Evolution of the depleted mantle: Hf isotope evidence from juvenile rocks through time. *Geochimica et Cosmochimica Acta* 63, 533–556.
- Willan, R.C.R., Pankhurst, R.J., Hervé, F., 1994. A probable Early Triassic age for the Miers Bluff Formation, Livingston Island, South Shetland Islands. *Antarctic Science* 6, 401–408.
- Williams, I.S., 1998. U–Th–Pb Geochronology by Ion Microprobe. In: McKibben, M.A., Shanks III, W.C., Ridley, W.I. (Eds.), *Applications of Micro-analytical Techniques to Understanding Mineralizing Processes. Reviews of Economic Geology* 7, 1–35.
- Willner, A.P., Sepúlveda, F.A., Hervé, F., Massonne, H.-J., Sudo, M., 2009. Conditions and Timing of Pumpellyite–Actinolite-facies Metamorphism in the Early Mesozoic Frontal Accretionary Prism of the Madre de Dios Archipelago (Latitude 50°20'S; Southern Chile). *Journal of Petrology* 50, 2127–2155.